

# Biophysical and formulation studies of the *Schistosoma mansoni* TSP-2 extracellular domain recombinant protein, a lead vaccine candidate antigen for intestinal schistosomiasis

Weiqliang Cheng<sup>1</sup>, Elena Curti<sup>2,3</sup>, Wanderson C Rezende<sup>2,3</sup>, Clifford Kwityn<sup>2,3,†</sup>, Bin Zhan<sup>2,3</sup>, Portia Gillespie<sup>2,3</sup>, Jordan Plieskatt<sup>4</sup>, Sangeeta B Joshi<sup>1</sup>, David B Volkin<sup>1</sup>, Peter J Hotez<sup>2,3,5</sup>, C Russell Middaugh<sup>1</sup>, and Maria Elena Bottazzi<sup>2,3,\*</sup>

<sup>1</sup>Macromolecule and Vaccine Stabilization Center; Department of Pharmaceutical Chemistry; University of Kansas; Lawrence, KS USA; <sup>2</sup>Departments of Pediatrics and Molecular Virology and Microbiology; National School of Tropical Medicine; Baylor College of Medicine; Houston, TX USA; <sup>3</sup>Sabin Vaccine Institute and Texas Children's Hospital Center for Vaccine Development; Houston, TX USA; <sup>4</sup>Department of Microbiology; Immunology and Tropical Medicine; the George Washington University; Washington, DC USA; <sup>5</sup>James A. Baker III Institute for Public Policy; Rice University; Houston, TX USA

<sup>†</sup>Current affiliation: Beckman Coulter Inc.; Chaska, MN USA

**Keywords:** schistosomiasis, *Schistosoma mansoni*, *Sm*-TSP-2, vaccine, neglected tropical diseases, tropical medicine, vaccinology

A candidate vaccine to prevent human schistosomiasis is under development. The vaccine is comprised of a recombinant 9 kDa antigen protein corresponding to the large extracellular domain of a tetraspanin surface antigen protein of *Schistosoma mansoni*, *Sm*-TSP-2. Here, we describe the biophysical profile of the purified, recombinant *Sm*-TSP-2 produced in the yeast *PichiaPink*<sup>™</sup>, which in preclinical studies in mice was shown to be an effective vaccine against intestinal schistosomiasis. Biophysical techniques including circular dichroism, intrinsic and extrinsic fluorescence and light scattering were employed to generate an empirical phase diagram, a color based map of the physical stability of the vaccine antigen over a wide range of temperatures and pH. From these studies a pH range of 6.0–8.0 was determined to be optimal for maintaining the stability and conformation of the protein at temperatures up to 25 °C. Sorbitol, sucrose and trehalose were selected as excipients that prevented physical degradation during storage. The studies described here provide guidance for maximizing the stability of soluble recombinant *Sm*-TSP-2 in preparation of its further development as a vaccine.

## Introduction

Schistosomiasis is one of the most important parasitic helminth infections of humans. Up to 400–600 million people may be infected with at least one species of schistosome,<sup>1</sup> with greater than 90% of the infections occurring in Africa; of these, the majority are caused by either *Schistosoma hematobium* or *Schistosoma mansoni* or by a co-infection of both.<sup>2</sup> *S. hematobium* causes approximately two-thirds of the cases in Africa and accounts for a disproportionate impact on girls and women, as it leads in many cases leading to female genital schistosomiasis and increased host susceptibility to acquiring HIV/AIDS.<sup>3</sup> The current approach to schistosomiasis control in Africa relies primarily on periodic and frequent mass drug administration with praziquantel, an approach that until recently has been hampered because of lack of access to this essential medicine. Following the January 2012 London Declaration for Neglected Tropical Diseases,<sup>4</sup> Merck KgaA has pledged to greatly expand

its praziquantel donations. Even with the prospect of widespread administration of praziquantel mass treatments, it is not expected that this approach will interrupt the transmission of human schistosomiasis, nor lead to the elimination of the disease as a public health problem.<sup>2</sup> Ultimately, the elimination of schistosomiasis from the African continent will likely require the development and delivery of a schistosomiasis vaccine, ideally one that would simultaneously target both *S. hematobium* (the cause of urogenital schistosomiasis) and *S. mansoni* (the cause of intestinal-hepatic schistosomiasis). To date, two candidate vaccines are in clinical trials, including Sh28GT targeting *S. hematobium* and Sm14 targeting *S. mansoni*.<sup>5,6</sup>

The Sabin Vaccine Institute Product Development Partnership (PDP) is developing a recombinant vaccine comprised of the extracellular domain of the *S. mansoni* tetraspanin surface antigen known as *Sm*-TSP-2 (Fig. 1). Proof of concept for the efficacy of the antigen in preclinical studies was summarized in a companion piece to this article (Curti et al., 2013,

\*Correspondence to: Maria Elena Bottazzi; Email: bottazzi@bcm.edu  
Submitted: 04/02/2013; Revised: 07/02/2013; Accepted: 07/17/2013  
<http://dx.doi.org/10.4161/hv.25788>

EFEKPKVKKHITSALKKLVDKYRNDEHVRKVFDEIQKQLHCCGADSPKDYGENP  
PTSCSKDGVQFTEGCIKKVSDLKAH

**Figure 1.** Amino acid sequence of the recombinant *Sm*-TSP-2 protein antigen.

accompanying article) and includes studies in mice challenged with *S. mansoni* cercariae and human immunological studies.<sup>7-9</sup> Tran et al., 2006, showed that the vaccination of mice with the recombinant proteins formulated with an equivalent volume of Freund complete or incomplete adjuvant followed by challenge infection with *S. mansoni* resulted in reductions of 57% and 64% (TSP-2) for mean adult worm burdens and liver egg burdens, respectively, over two independent trials.<sup>8</sup>

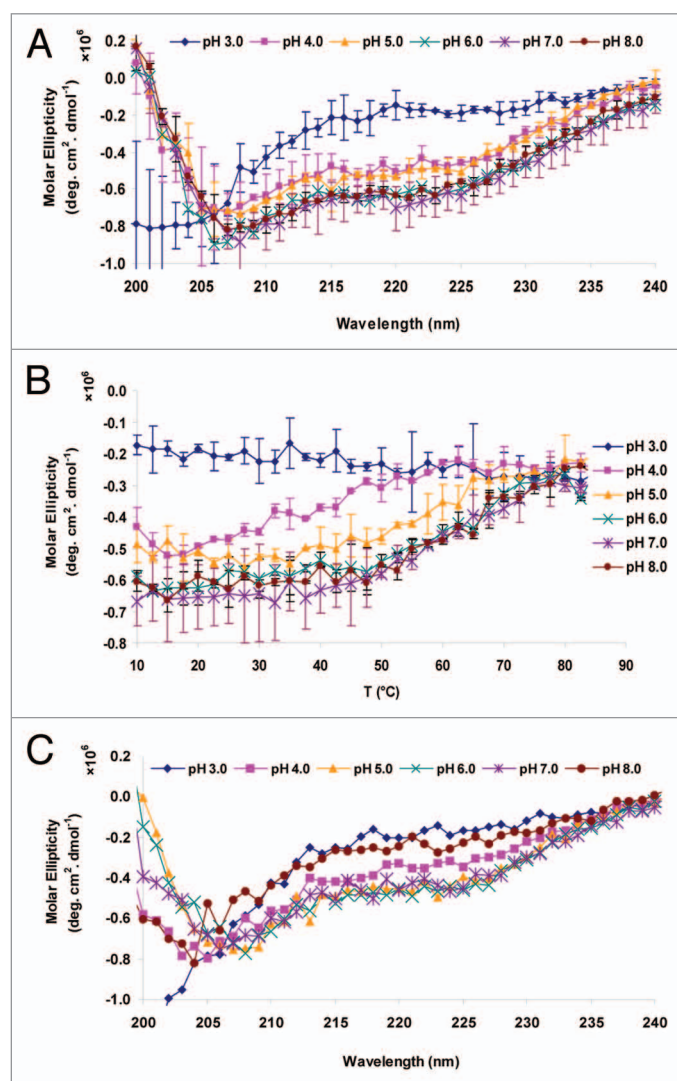


**Figure 2.** Circular dichroism analysis of *Sm*-TSP-2 as a function of solution pH and temperature. (A) Averaged CD Spectra of *Sm*-TSP-2 at 10 °C before thermal treatment (n = 2). Error bars are from duplicate measurements. (B) Average Ellipticity of *Sm*-TSP-2 at 222 nm as a function of temperature (n = 2). Error bars are from duplicate measurements. (C). Average CD Spectra of *Sm*-TSP-2 at 10 °C after thermal treatment (n = 2). The error bars were removed.

*Sm*-TSP-2 elicited an endpoint IgG1 and IgG2a titer in excess of 1:1 600 000 for IgG1 and 1:1 400 000 for IgG2a as evaluated by ELISA.<sup>8</sup> Simultaneously, it was shown that the level of IgG1 and IgG3 were significantly high in individuals that were putative resistant, and chronically infected, compared with individual that had never been exposed to *Schistosoma* infection. Additional studies are underway to determine whether immunization with *Sm*-TSP-2 will cross protect against *S. hematobium* challenge infections. The *Sm*-TSP-2 vaccine consists of the 9 kDa large extracellular domain of *Schistosoma mansoni* TSP-2 protein, which is formulated on an aluminum salt adjuvant, together with a synthetic Toll-like receptor 4 agonist. Aluminum based hydrated gels, namely aluminum hydroxide and aluminum phosphate are by far the most widely used, licensed for human use, adjuvants.<sup>10</sup> A number of biophysical analyses specifically looking at the structure of model antigens bound to aluminum based hydrated gels, have revealed none or subtle effects upon the bound protein.<sup>11-16</sup> Even though alum adjuvantation is not expected to affect the properties of *Sm*-Tsp-2, future studies will be able to address and document that this indeed is the case.

In the companion paper (Curti et al., 2013), the 20L scale up expression and fermentation of the soluble recombinant *Sm*-TSP-2 in the yeast *PichiaPink*<sup>TM</sup>, followed by the purification (to a purity of > 97% and yield of recovery of > 30%), is described. Critical to the development of the *Sm*-TSP-2 schistosomiasis vaccine are studies aiming to identify optimal buffer conditions, such as pH, and excipients, which can maximize the long-term storage stability of the recombinant antigen.

In this manuscript, we provide a summary of a series of biophysical profiling studies performed on the yeast-expressed *Sm*-TSP-2 extracellular loop recombinant protein to develop a suitable formulation that would provide long-term storage stability of the antigen while permitting compatibility with and binding to an aluminum based adjuvant. In addition, these studies also provide important protein physical stability information that is useful for process development and scale-up efforts. Taken together, the overall aim is to ultimately ensure a consistent, reproducible formulation of a stable recombinant protein vaccine.

## Results

### Analytical and biophysical characterization of the recombinant *Sm*-TSP-2 protein

Process development of any recombinant protein relies on a robust portfolio of assays for product characterization (e.g., appearance, identity, integrity, and purity), identification of contaminants and evaluation of stability, all performed according to a quality control program. The process development strategy to produce the recombinant *Sm*-TSP-2 extracellular loop protein included a 20L scale fermentation, and two-step chromatography purification as described in detail in the accompanying Curti et al., 2013. The purified protein had an estimated purity of 97%, and was stored frozen at -80 °C in a solution consisting of 10 mM Imidazole, 15% sucrose and 2 mM phosphate at pH 7.4. A broad range of assays were used for the purpose of

characterizing the protein antigen, including multiple methods for identity (Immunoblot, N-terminal sequencing, mass spectrometry, amino acid analysis), integrity (SDS-PAGE and RP-HPLC) as well as purity (SDS-PAGE, host cell protein assay) as described in detail in Curti et al., 2013. The amino acid sequence of the recombinant *Sm*-TSP-2 extracellular loop protein is shown in **Figure 1**.

To ensure that the conditions of maximum protein physical stability were known and chosen for long-term storage of *Sm*-TSP-2, a comprehensive approach to the physical characterization and stabilization of the vaccine antigen was undertaken. Collectively, these studies provide specific information concerning the physical state of the protein as a function of temperature and pH. The data gathered from such methods and techniques were then used to generate an empirical phase diagram of *Sm*-TSP-2, which describes in the form of a colored map the higher-order structural integrity and conformational stability of the *Sm*-TSP-2 protein. This empirical phase diagram approach has also been used to generate conformational stability information on several other vaccine antigens as well as with other conditions that can stress the structural integrity of protein molecules, such as protein concentration and ionic strength as a function of temperature.<sup>15-19</sup>

#### Circular dichroism, CD

Changes in secondary structure of the *Sm*-TSP-2 proteins were studied by monitoring the change in the far UV-CD signal as a function of both pH and temperature.

**Figure 2A** shows the pH dependence of the secondary structure of the *Sm*-TSP-2 extracellular loop protein at 10 °C. In general, a broad peak from 200 to 240 nm was observed for most of the pH values examined suggesting a mixture of secondary structure types. At pH 6.0–8.0 and 10 °C, the protein shows two negative peaks at approximately 207 nm and 223 nm, a typical feature of  $\alpha$ -helical structure and content. The CD spectra of the protein at pH 4.0 and 5.0 did not vary significantly from the one measured at pH 6.0–8.0, with respect to the molar ellipticity at 205–240 nm (**Fig. 2A**) In contrast, the CD spectrum of the protein at pH 3.0 was significantly different, indicating that the secondary structure was altered at this pH even at low temperature. **Figure 2B** shows the molar ellipticity of *Sm*-TSP-2 at 222 nm as a function of temperature. At pH 6.0 to 8.0, the *Sm*-TSP-2 protein manifests a gradual decrease of ellipticity starting from 45 °C, while at pH 4.0 and 5.0, the structural transition temperature started at approximately 20–40 °C, much lower than that at pH 6.0–8.0. At pH 3.0, there was little to no change in the CD signal at 220 nm as a function of temperature probably due to the already fully altered and unfolded structure of the protein

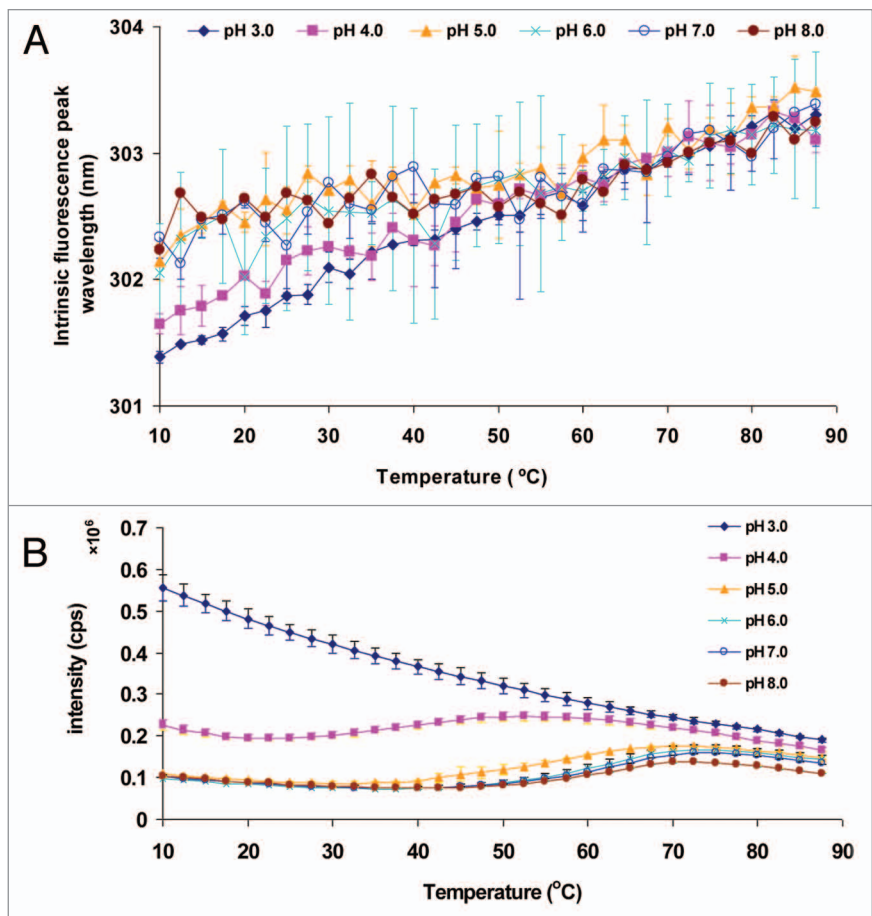


**Figure 3.** Intrinsic fluorescence spectroscopy analysis of *Sm*-TSP-2 as a function of solution pH and temperature. Tyrosine fluorescence peak position (**A**) and intensity (**B**) of *Sm*-TSP-2 as function of pH and temperature. Solutions containing *Sm*-TSP-2 at indicated pH values were heated from 10–87.5 °C and the fluorescence emission maximum was determined after excitation at 280 nm. Error bars are from duplicate measurements.

even at low temperatures (e.g., 10 °C). At higher temperatures (75–80 °C) and pH 4.0–8.0, *Sm*-TSP-2 showed low ellipticity values across the entire pH range indicating that under these conditions, the protein is fully unfolded. After thermal treatment of the sample at 87.5 °C followed by cooling the sample down to 10 °C, the CD spectra appeared to be different from those of untreated samples, as shown in **Figure 2C**, indicating that the alterations in protein structure by exposure to elevated temperature were not reversible.

#### Fluorescence and light scattering studies

##### Intrinsic fluorescence

Changes in the tertiary structure of the *Sm*-TSP-2 protein were monitored by analyzing changes in the intrinsic fluorescence emission peak position (**Fig. 3A**) and in the fluorescence peak intensity (**Fig. 3B**) as a function of pH and temperature. Because tryptophan residues are not present in the *Sm*-TSP-2 extracellular loop primary structure, and there are two tyrosine residues in *Sm*-TSP-2 sequence, tyrosine was used as a probe despite its relative insensitivity to local environmental change. A subtle red shift of the tyrosine peak was observed with increasing

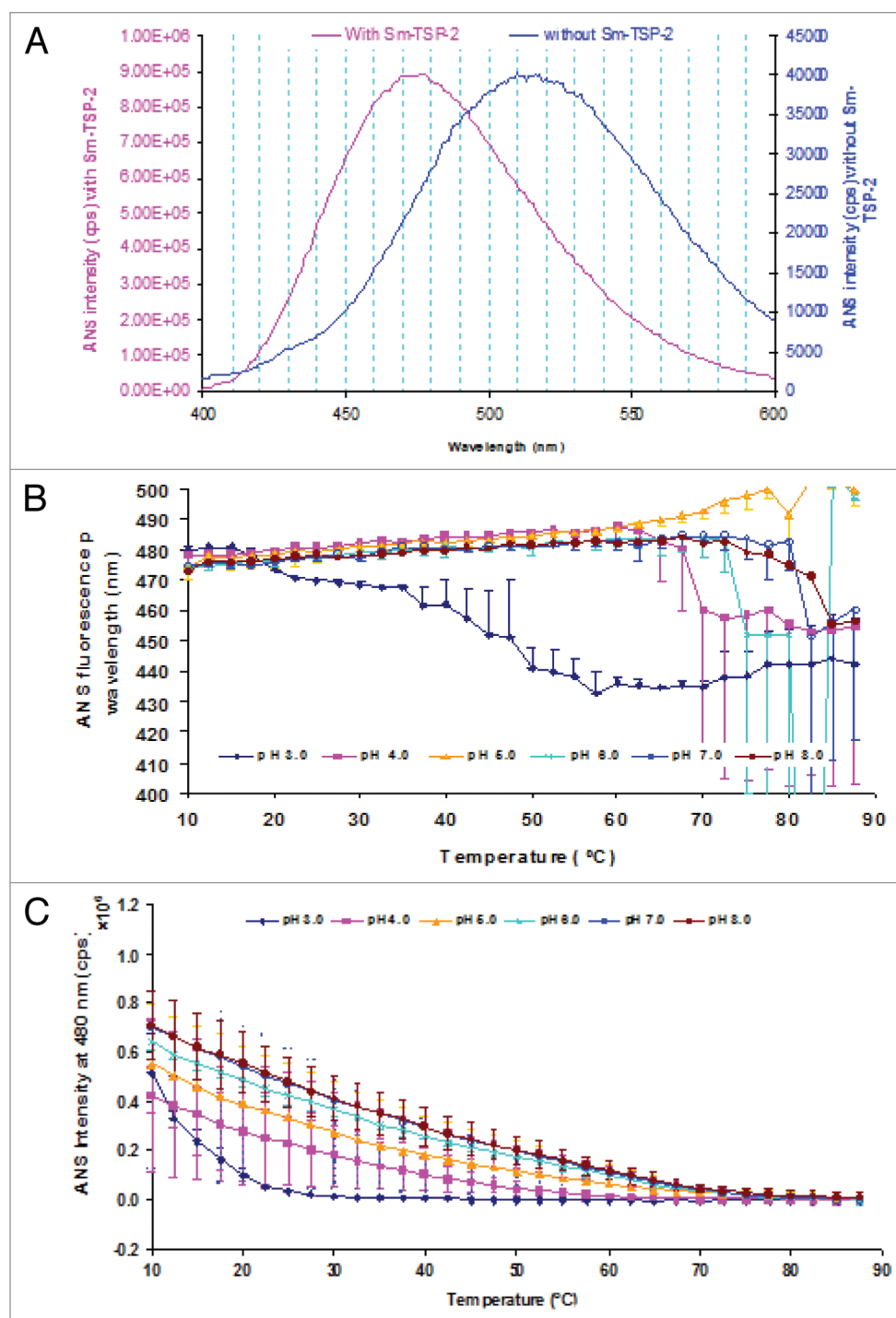


**Figure 4.** Extrinsic ANS fluorescence spectroscopy analysis of *Sm-TSP-2* as a function of pH and temperature. Representative ANS fluorescence emission spectra in the presence and absence of *Sm-TSP-2* at 10 °C (A), ANS peak wavelength (B) and ANS intensity at 480 nm upon binding to *Sm-TSP-2* as a function of temperature. Error bars are from duplicate measurements.

temperature at all pH conditions examined, suggesting that the phenol side chains were exposed to a more polar environment upon thermal unfolding. The tyrosine peak position was at lower wavelength at pH 3.0 and 4.0 than that at pH 5.0–8.0, suggesting that the tyrosine residues were overall exposed to a less polar microenvironment at pH 3.0–4.0. Though the peak

shifts for tyrosine fluorescence across the different pH conditions and temperatures were very small, the trend appears to be clear. This magnitude of the peak shifts for tyrosine fluorescence as well as ANS fluorescence (see below), however, could be related to its small size and high hydrophilicity and is not expected to be routinely observed for most large and hydrophobic proteins.

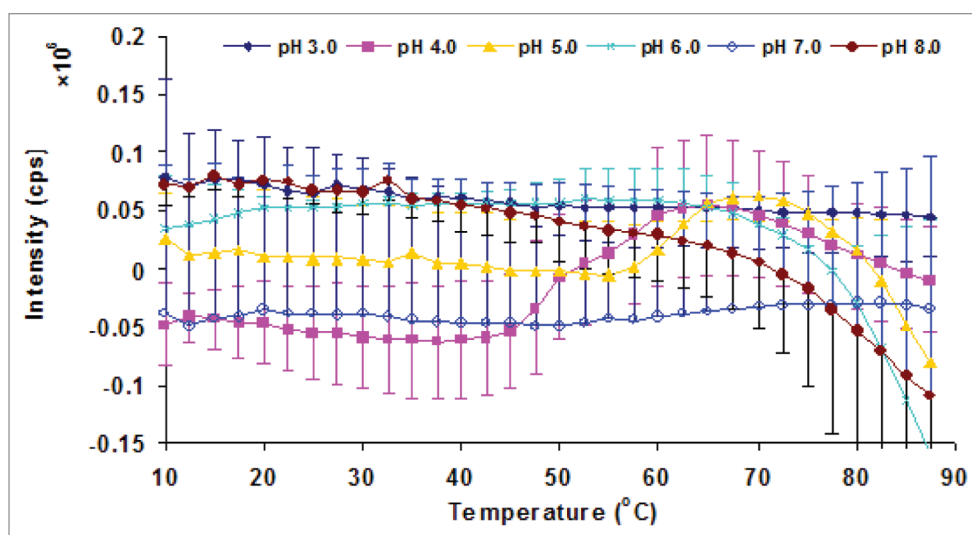


**Figure 5.** Static light scattering of *Sm-TSP-2* solutions as a function of pH and temperature. *Sm-TSP-2* was heated from 10 to 87.5 °C and the scattering intensity was monitored at 280 nm. Error bars are from duplicate measurements.

Nonetheless, there were no obvious thermal transitions observed under the solution conditions tested. Peak intensity data (Fig. 3B), however, shows a clear, but gradual, pH dependent transition. The initial decrease of fluorescence peak intensity is presumably due to the well-known intrinsic effect of temperature on fluorescence quantum yield and internal non-radiative thermal conversion processes.<sup>20</sup> At pH 3.0, there was no clear structural transition. A transition was, however, observed at pH 4.0–8.0. The  $T_m$  of the transition was approximately 60 °C for pH 6.0–8.0, 55 °C for pH 5.0, and 37.5 °C for pH 4.0, respectively.

#### ANS fluorescence

Extrinsic fluorescence using the fluorescent probe ANS is often employed to study changes in tertiary structure of proteins as a function of temperature. ANS fluorescence is quenched in aqueous solutions, while its intensity increases in apolar environments.<sup>21</sup> Interpretation of structural changes can, however, be complicated by electrostatic interactions of the negatively charged sulfonate group of ANS with positive charged amino acid residues within proteins, such as lysine, arginine and histidine.<sup>22,23</sup> Nevertheless, ANS is often used as an indicator of the exposure of hydrophobic regions upon conformational perturbation of a protein. Since ANS binds to apolar sites in a protein, an increase in the fluorescence intensity of the emission maximum, accompanied by a blue shift in the peak position, is frequently observed. Figure 4A shows representative ANS fluorescence spectra of ANS in the presence and absence of 0.2 mg/mL *Sm-TSP-2* protein. The fluorescence emission peak position was around 475–480 nm and 510–520 nm, respectively, in the presence and absence of *Sm-TSP-2*, indicating that ANS did bind to the protein and the binding of ANS to *Sm-TSP-2* is at least partially due to hydrophobic interactions.<sup>21</sup> The fluorescence spectra as a function of temperature overall paralleled each other with small peak shift (data not show). Instead of a blue shift, the ANS fluorescence peak position at pH 4.0–8.0 showed a slight red shift along with increases in temperature (Fig. 4B). This slight red shift in fluorescence peak position as

the temperature increased may be due to a decreasing number of ANS molecules bound to *Sm-TSP-2* rather than the decreasing fluorescence quantum yield of a constant number of bound ANS molecules. This assumption is consistent with the observation that ANS fluorescence intensity (Fig. 4C) increased less in the presence of *Sm-TSP-2* in comparison with other proteins. The smaller difference for ANS fluorescence intensity in the presence and absence of the protein could also be reflected by the relatively larger error bars, suggesting the presence of the protein resulted in only relatively small changes in ANS fluorescence quantum yield. Increases in temperature resulted in the peak intensity of ANS in the presence of *Sm-TSP-2* becoming slightly higher or comparable to the peak intensity of the buffers (Fig. 4C). At low ANS intensity in the presence of *Sm-TSP-2* when the temperature increased, the peak wavelength data was not reliable. Unlike the ANS intensity profiles as a function of temperature at pH 4.0–8.0, ANS peak intensity at pH 3.0 decreased more rapidly when the temperature increased from 10 to 20 °C, indicating that the binding of ANS to *Sm-TSP-2* was affected more by temperature compared with other pH conditions. A possible reason for this observation is that the structure of *Sm-TSP-2* at 10 °C at pH 3.0 might be less favorable than that at pH 4.0–8.0 for ANS binding. For all pH values tested, ANS intensity gradually decreased to zero probably due to weak binding of protein-ANS complex along with decreasing fluorescence quantum yield while the temperature increased although no obvious structural transition was observed.

#### Light scattering

The temperature dependent static light scattering of *Sm-TSP-2* under different pH conditions was also measured (Fig. 5). The static light scattering intensity of *Sm-TSP-2* after subtraction from that of buffer was overall very weak. Furthermore, given the low scattering intensity and experimental error, no significant increase in scattering intensity was observed across the entire pH and temperature range, indicating that *Sm-TSP-2* at 0.2 mg/mL did not notably aggregate when heated in the pH range of 3–8.

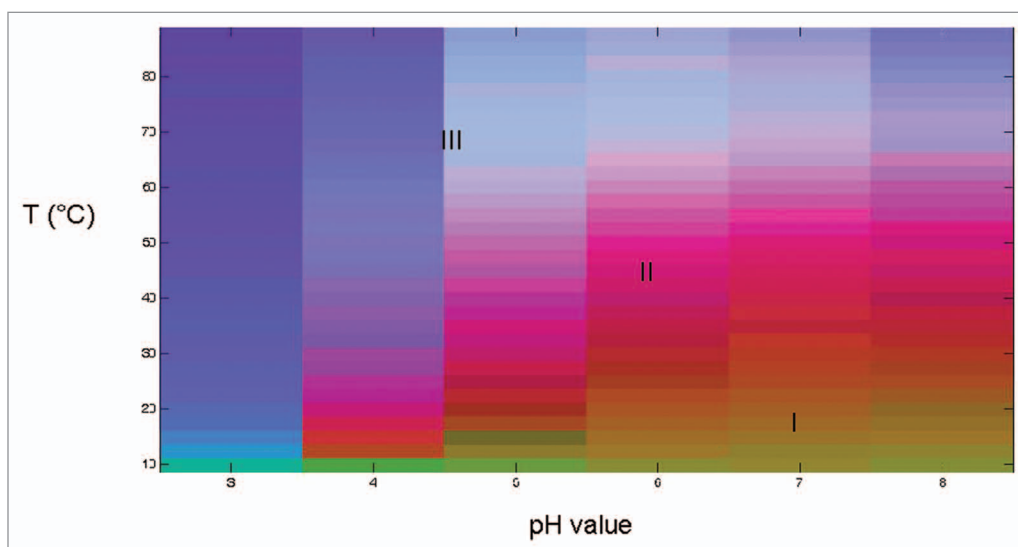


**Figure 6.** Empirical Phase Diagram of *Sm-TSP-2*. A combination of circular dichroism, tyrosine fluorescence intensity and ANS fluorescence intensity data were used to generate an empirical phase diagram. Region I represents the protein in its native folded state, Region II is a partially structurally altered state, while Region III is an extensively structurally altered state due to thermal unfolding events.

#### Empirical phase diagram

An empirical phase diagram (EPD) was created using a combination of the biophysical data described above to produce an overall picture of *Sm-TSP-2* conformational stability as a function of temperature and pH (Fig. 6). Using this approach, the spectral data from the multiple characterization methods (CD, tyrosine fluorescence intensity, and ANS fluorescence intensity) are graphically represented using a multi-dimensional vector space. Since no aggregation was observed, the light scattering data were not used. For every combination of pH and temperature at which measurements were taken, a 3-dimensional vector was created. The assignment to the components of each vector of a different color (red, green, and blue) produces a combined unique color. Analysis of the EPD leads to the identification of several different apparent phases or stability regions. Regions of continuous color represent similar structural states while abrupt changes in color can be used to identify changes in the physical state of the protein due to temperature or pH stress. For *Sm-TSP-2*, the EPD could be divided into three well defined regions (Fig. 6). The first phase (Region I) displayed in orange-green color and represents the protein in its native folded state. This region encompasses mainly pH 6.0 to 8.0 in the temperature range of 10 to 25 °C. The major unfolding events begin around 35 °C at pH 7.0 and 8.0, and at lower temperatures at pH values below 6.0. In Region II, the *Sm-TSP-2* protein exists in partially structurally altered states as shown in purple, which spans across all pH conditions at temperatures ranging from 12.5 °C at pH 4.0 to 65 °C at pH 8.0. The third phase (Region III) represents an extensively structurally altered state due to thermal unfolding events. Overall, the EPD of *Sm-TSP-2* shows relatively better conformational stability at higher pH (6.0–8.0) with the highest thermal stability observed at pH 7.0 and 8.0. Within this pH range the folded state was maintained up to a temperature of approximately 35 °C. The structural transition temperature, even under the most stable pH

condition, is far lower than that of many proteins,<sup>24,25</sup> indicating that *Sm-TSP-2* requires precise conditions to ensure stability.

#### Excipient screening to improve protein physical stability

The biophysical profiling data obtained above was used to design a high-throughput screening assay for the identification of potential excipient based stabilizers for *Sm-TSP-2*. It is often the case that optimization of solution pH and buffering species alone is not sufficient to ensure long-term stability of a vaccine protein antigen. Therefore, identification of stabilizing excipients is also required. Compounds were defined as having a stabilizing effect when they increased the thermal melting temperature ( $T_m$ ) values of the first structural transition, as seen in the empirical phase diagram of the protein, which is often correlated with storage stability.<sup>26</sup> Screening employed a library of GRAS compounds. The conditions of the screening were determined by inspection of the apparent phase boundaries established by the EPD. A solution pH of 7.0 was selected as the optimum pH of this protein since higher pH often results in unfavorable chemical degradation such as deamination,<sup>27,28</sup> and pH 7.0 was therefore used to evaluate if excipients could further improve physical stability of *Sm-TSP-2* under thermally stressed condition (i.e., the structural transition of the protein at this pH initiates at higher temperature). To this end, the intrinsic fluorescence of *Sm-TSP-2* as a function of temperature in the presence of excipients was monitored as a function of excipient type and concentration. Figure 7 and Table 1 show respectively the normalized tyrosine fluorescence intensity of *Sm-TSP-2* as a function of temperature and the corresponding  $T_m$  values when formulated with various compounds. The fluorescence intensity profiles as a function of temperature for each excipient were parallel to each other except for Brij-35. The reason Brij-35 manifested a different intensity profile is not currently known. It might be related to its micelle status as a function of temperature which results in a different fluorescence quenching mechanism

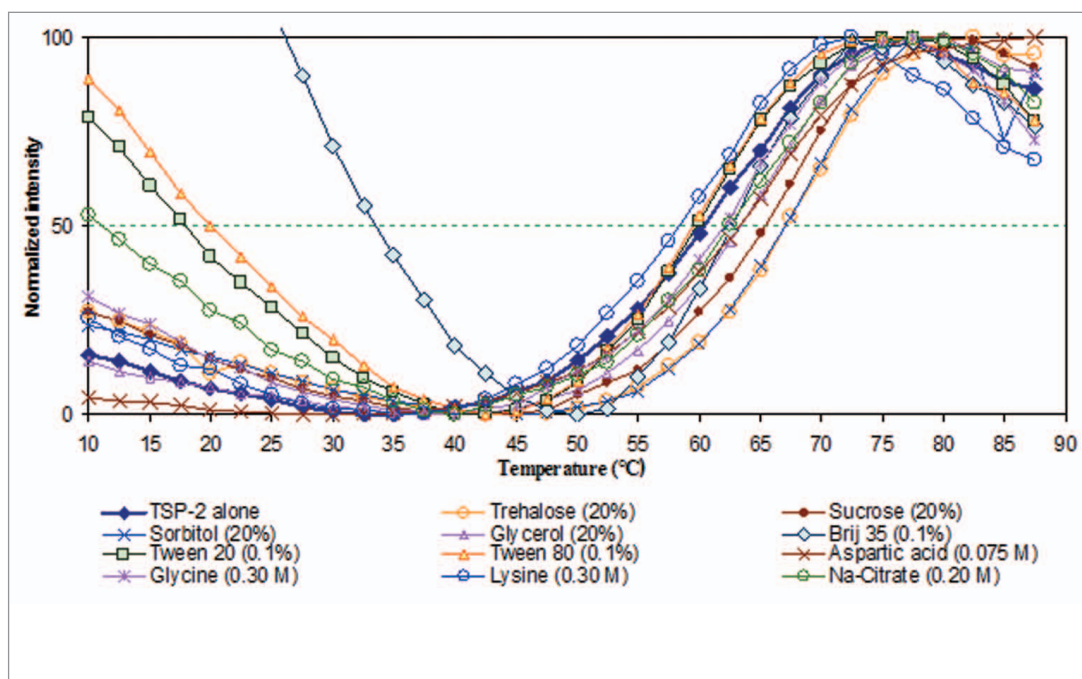


**Figure 7.** Normalized average Tyr fluorescence intensity of *Sm*-TSP-2 formulated with indicated excipients (type and concentration) in 10 mM imidazole buffer at pH 7.0 containing 145 mM NaCl. Replicates were  $n = 2$ , but the error bars were removed for a clear presentation of the data.

other than temperature induced internal conversion. *Sm*-TSP-2 in 20 mM of imidazole buffer at pH 7.0 showed a  $T_m$  value at 60.3 °C. In the presence of 20% sorbitol, trehalose and sucrose, the  $T_m$  value increased by 5.0–7.8 °C, and were among the most effective stabilizers identified in this study (Table 1). Among these excipients, sucrose can potentially hydrolyze releasing dextrose and fructose during long-term storage (especially at lower pH). As a reducing sugar, dextrose can potentially react with the free amine side chain at the N-terminal of *Sm*-TSP-2 as well as with the amino group of lysine residues (Malliard reaction).<sup>29–31</sup> Arginine and guanidine hydrochloride decreased the  $T_m$  value by 6.4 and 12.3 °C, respectively. These compounds are therefore considered to be strong destabilizers of *Sm*-TSP-2. These results are consistent with the results of many similar studies with other protein molecules.<sup>25,32,33</sup> Glycerol appeared to be a potential stabilizer; however, due to its much higher osmolarity at a comparable weight amount of sugar molecule, it was not further pursued as a stabilizer. Less effective stabilizing effects were observed for aspartic acid, possibly due to charge-charge interactions between the positive charged side chains of the antigen and the negatively charged carboxylic groups. Brij 35 appeared to stabilize the antigen better than other surfactants, such as Tween-80 and Tween-20. The different effects of various non-ionic surfactants is consistent with an earlier study with the EBA-175 RII-NG antigen, a candidate for a malaria vaccine.<sup>24</sup> Other excipients, such as glycine and lysine, had little effect on the physical stability of *Sm*-TSP-2.

The stabilizing effect of trehalose, sorbitol, Brij-35, and sodium citrate as a function of their concentrations was further examined. Table 2 shows that trehalose and sorbitol have

a concentration dependent stabilization effect with higher concentrations producing increased physical stabilization of *Sm*-TSP-2. Other stabilizers, such as Brij-35 and sodium citrate at different concentrations show a less obvious concentration-dependent effect. A further study concerning the effect of a combination of Brij-35 with 10% trehalose and sorbitol suggested that Brij 35 might have a slight additive effect on the stabilization of *Sm*-TSP-2 (Table 3). Sugars like sorbitol and trehalose as well as Brij-35, are unlikely to interfere with the adsorption to Alhydrogel<sup>®</sup>,<sup>24</sup> an aluminum adjuvant currently under consideration for use in a final formulation. In contrast, sodium citrate at pH 7.0 could reduce the positive charge on the surface of the aluminum adjuvant and potentially result in decreased binding of the antigen to the adjuvant. Therefore, the use of sodium citrate in combination with other stabilizing excipients was not further explored.

## Discussion

Developing a vaccine candidate is a complex and costly undertaking. Because of the complexity in manufacturing vaccine products, it is important to have a good understanding of environmental factors that can enhance efficacy, safety and stability of the vaccine antigen even at the early stages of process development. A key consideration in ensuring long-range success in stability testing is a rational approach for the development of a robust antigen formulation which includes comprehensive biophysical characterization of the antigen and identification of optimum pH and excipients that can maximally stabilize the antigen. This approach was previously successful for optimizing

**Table 1.** Thermal unfolding temperature ( $T_m$ ) values of *Sm*-TSP-2 formulated in at pH 7.0 with indicated excipients (type and concentration) as measured by normalized tyrosine fluorescence intensity of *Sm*-TSP-2 formulated with excipients

Excipients	Concentration	$T_m$ average (n = 2)	$\delta T_m$	SD
Dextrose	20.0%	68.1	68.1	0.8
Trehalose	20.0%	67.1	67.1	0.1
Sorbitol	20.0%	67.1	67.1	0.6
Lactose	20.0%	66.8	66.8	0.0
Sucrose	20.0%	65.3	65.3	0.1
Mannitol	10.0%	63.9	63.9	0.9
Aspartic acid	0.075 M	63.5	63.5	1.6
Glycerol	20.0%	63.3	63.3	0.4
Brij 35	0.10%	62.6	62.6	0.1
Sodium citrate	0.20 M	62.5	62.5	0.0
Glycine	0.30 M	62.1	62.1	0.0
Glutamic acid	0.15 M	62.0	62.0	0.7
Malic acid	0.15 M	60.8	60.8	0.0
Lactic Acid	0.15 M	60.8	60.8	0.1
Protein alone		60.3	60.3	0.0
Proline	0.30 M	60.0	60.0	0.4
Tween 20	0.10%	59.9	59.9	0.2
Dextran T70	Molar ratio 0.1	59.7	59.7	0.0
Dextran T70	Molar ratio 1.0	59.6	59.6	0.1
Tween 80	0.10%	59.5	59.5	0.4
Dextran T70	Molar ratio 2.5	59.4	59.4	0.3
Pluronic F-68	0.10%	59.4	59.4	0.2
Arginine/Glutamic acid	0.075 M	58.9	58.9	0.4
Lysine.HCl	0.30 M	58.4	58.4	0.9
Calcium chloride	0.015 M	58.0	58.0	0.3
2-OH propyl $\beta$ -CD	10.0%	56.4	56.4	0.3
$\alpha$ Cyclodextrin	2.50%	56.2	56.2	0.7
Dietanolamine	0.30 M	56.1	56.1	0.6
2-OH propyl $\beta$ -CD	10.0%	55.0	55.0	0.4
Arginine	0.30 M	53.9	53.9	1.3
Guanidine.HCl	0.30 M	48.0	48.0	1.4

the stability of EBA-175 RII-NG, a malaria vaccine<sup>24</sup> and a human hookworm vaccine antigen,<sup>34</sup> which is now in clinical trials.

Using a similar approach, the ongoing development of *Sm*-TSP-2 recombinant protein subunit vaccine antigen has included a comprehensive biophysical characterization of the antigen. These studies were focused on identifying an optimal pH and excipients that enhanced the thermal stability of the antigen. An empirical phase diagram approach was undertaken not only to better visualize and identify the optimal pH conditions, but also as a starting point to screen conditions, a library of GRAS compounds was evaluated for their potential to further stabilize *Sm*-TSP-2.

Multiple biophysical techniques that monitor conformational alterations at the secondary and tertiary structure level, upon changes in temperature and pH, were adopted to study the impact of these parameters on the stability of *Sm*-TSP-2. CD, intrinsic fluorescence and extrinsic ANS fluorescence were used to monitor protein stability and these large data sets were summarized and visualized by constructing an empirical phase diagram. The EPD generated for *Sm*-TSP-2 clearly indicated that the protein's extracellular loop is in its native conformation from pH 6.0–8.0, while its conformational stability significantly decreased below pH 5 to an extensively unfolded state at pH 3.0. The conformational stability of *Sm*-TSP-2 was very sensitive to temperature. The native folded state was maintained from

**Table 2.** Summary of thermal unfolding temperature ( $T_m$ ) values for *Sm*-TSP-2 formulated at pH 7.0 with different concentrations of candidate stabilizers ( $n = 2-3$ ) as measured by of normalized tyrosine fluorescence intensity

Excipients	Conc.	$T_m$ (°C)	SD (°C)	$\Delta T_m$ (°C)
trehalose	20.0%	67.2	0.9	6.8
	15.0%	65.6	0.2	5.2
	10.0%	63.3	0.7	2.9
	7.5%	62.4	0.4	2.0
Sorbitol	20.0%	67.2	0.6	6.8
	15.0%	64.6	0.6	4.2
	10.0%	63.3	0.3	2.9
	7.5%	63.0	0.8	2.6
Brij-35	0.10%	62.5	0.0	2.1
	0.05%	61.8	0.3	1.4
	0.01%	61.6	0.1	1.2
Sodium citrate	0.20 M	62.5	0	2.1
	0.10 M	60.1	0.5	-0.3
	TSP-2 Alone	60.4	0.2	0.0

pH 6.0 to 8.0 up to only 30 °C, while pH 7.0 appeared to be an acceptable pH condition when the potential for chemical instability is also taken into account.

A wide variety of compounds were used to screen for stabilizing agents. Each excipient was individually tested for its ability to stabilize the protein's structure against thermal stress. A high throughput intrinsic protein fluorescence based spectroscopic assay was developed and utilized for this purpose. A number of compounds stabilized the *Sm*-TSP-2 extracellular loop protein in its native conformation. These compounds primarily belonged to the class of sugars and polyols, with sucrose, trehalose and sorbitol ranking among the best candidates. The stabilizing effect of sugars on proteins is generally thought to be due to preferential exclusion, which results in the smallest, more thermodynamically favorable, surface area of a more ordered native structure with lower conformational mobility in the presence of sugars.<sup>35-37</sup> These sugars have been exploited extensively as pharmaceutical excipients in liquid as well as lyophilized formulations of therapeutic proteins.<sup>35,36,38,39</sup> Although sucrose can slowly hydrolyze to fructose and glucose under acidic conditions, potentially leading to non-enzymatic glycation of proteins, this degradation pathway could be a lesser concern in a *Sm*-TSP-2 formulation if it is formulated at neutral pH and/or subsequently lyophilized to a dried cake at a low water content.<sup>27</sup> Sorbitol and trehalose appeared to be better alternatives as stabilizing excipients, since they are unlikely to display chemical reactivity of sucrose, yet have comparable ability to physically stabilize *Sm*-TSP-2.

In summary, this pre-formulation characterization study was conducted to better understand the physical stability of *Sm*-TSP-2 as a function of pH and temperature, and to identify excipients that can potentially improve the long-term storage stability of the antigen. *Sm*-TSP-2 is a relatively unstable protein in solution with structural transitions occurring at ambient or slightly elevated

**Table 3.** Effect of 10% trehalose or 10% sorbitol on the thermal unfolding temperature  $T_m$  values of *Sm*-TSP-2 in the presence or absence of 0.1% Brij 35 at pH 7.0 in 20 mM imidazole buffer as measured by normalized tyrosine fluorescence intensity measurements

Formulation		$T_m$ (°C)	SD
10.0% trehalose	0.1% Brij 35	64.0	0.3
	-	63.3	0.7
10.0% Sorbitol	0.1% Brij 35	64.2	0.4
	-	63.3	0.3

temperatures, depending on solution pH. *Sm*-TSP-2 at pH 6.0–8.0 exhibited enhanced conformational stability compared with lower pH values such as 4.0 to 5.0. *Sm*-TSP-2 is least stable at pH 3.0 with structurally altered protein observed even at low temperatures. Screening for stabilizing excipients found that sorbitol and trehalose are among the best compounds for further improving the stability of *Sm*-TSP-2. Sorbitol and trehalose displayed a concentration dependent stabilization effect. When 0.1% Brij-35 was combined with 10% sorbitol and trehalose, a slight additive stabilization effect was seen. Overall, these results provide comprehensive picture of the physical stability of *Sm*-TSP-2 as a function of pH and temperature, and provide useful information for further formulation development of *Sm*-TSP-2 as a promising anti-schistosomiasis vaccine.

## Materials and Methods

### Expression and purification of the *Sm*-TSP-2 recombinant protein

The DNA sequence of the large extracellular domain of *Sm*-TSP-2 was codon optimized for expression in *PichiaPink*<sup>TM</sup> as previously described.<sup>8</sup> A two-step chromatography process was used to purify the *Sm*-TSP-2 protein, which includes a strong cation exchange SP Sepharose XL column (GE healthcare) and a Q Sepharose HP anion exchange resin (GE healthcare). While SP Sepharose XL resin was selected as for actively binding the *Sm*-TSP-2 protein and removing the host cell proteins and low molecular weight product derived contaminants, the Q Sepharose HP medium was used as a negative capture resin during this process. Details of the expression, purification and analytical characterization of *Sm*-TSP-2 (with an estimated purity of 97%) are provided in the accompanying paper.

### Biophysical characterization and profiling

#### Sample and buffer preparation

Purified *Sm*-TSP-2 was stored frozen at -80 °C in a solution containing 10 mM imidazole, 10% sucrose and 2 mM phosphate at pH 7.4 at approximately 1 mg/mL. Samples were thawed at room temperature and dialyzed with a dialysis cassette (MWCO 3K, Millipore) against 20 mM citrate-phosphate buffers at different pH values, but at a constant ionic strength of 0.15, obtained by altering the amount of sodium chloride added. Buffers at pH values ranging from 3 to 8 were obtained by mixing 0.4 M citric acid and sodium phosphate dibasic stock solutions in different ratios. After dialysis, the absorbance of *Sm*-TSP-2 was measured at 280 nm, and the protein concentration

was determined using a theoretical extinction coefficient of  $8312 \text{ M}^{-1}\text{cm}^{-1}$ . The protein was then diluted to  $0.2 \text{ mg/mL}$  with the respective buffers in the pH range of 3–8 in one pH unit increments.

#### *Circular dichroism (CD) spectroscopy*

CD spectra were obtained using a Jasco J-810 spectropolarimeter equipped with a Peltier controlled 6-position cell holder. Spectra from 260 to 190 nm were collected at temperature increment of  $2.5 \text{ }^\circ\text{C}$  with the temperatures ranging from a minimum of  $10 \text{ }^\circ\text{C}$  to a maximum of  $87.5 \text{ }^\circ\text{C}$ . A temperature ramp rate of  $2.5 \text{ }^\circ\text{C}/\text{min}$  and an incubation time of 120 sec were used. Measurements were taken using a  $0.1 \text{ cm}$  path length quartz cuvette, with a scanning speed of  $50 \text{ nm}/\text{min}$  and a resolution of  $1 \text{ nm}$ . The CD data were converted into molar ellipticity after subtracting signals from buffer blanks at each pH. The CD signals at  $222 \text{ nm}$  were extracted and plotted as an indicator of change in secondary structure as a function of temperature. After a thermal treatment at  $87.5 \text{ }^\circ\text{C}$ , the CD spectra were measured again at  $10 \text{ }^\circ\text{C}$  to monitor reversibility.

#### *Static light scattering and intrinsic fluorescence spectroscopy*

Static light scattering intensities and intrinsic tyrosine fluorescence spectra were acquired using a Photon Technology International (PTI) spectrofluorometer equipped with a turreted four-position Peltier-controlled cell holder and a xenon lamp. Since there are no tryptophan residues present in the *Sm-TSP-2* protein, the overall intrinsic fluorescence of the two tyrosine residues was monitored. An excitation wavelength of  $280 \text{ nm}$  at a slit width set at  $1.0 \text{ nm}$  was used, and emission spectra from  $285\text{--}385 \text{ nm}$  at a slit width set at  $1.0 \text{ nm}$  were collected by a photomultiplier at right angle to the excitation radiation. A second photomultiplier, placed at  $180^\circ$  to the emission detector was used to record light scattering intensity from  $275\text{--}375 \text{ nm}$  at slit width of  $0.2 \text{ nm}$ . A rectangular cuvette ( $10 \times 10 \text{ mm}$ ) containing  $1.0 \text{ ml}$  of sample was used. Spectra were obtained at  $2.5 \text{ }^\circ\text{C}$  intervals at temperatures ranging from  $10\text{--}87.5 \text{ }^\circ\text{C}$ . The spectrum of the corresponding buffer was subtracted from the spectra of each protein prior to data analysis using Microsoft Excel software. Fluorescence intensity and peak positions were obtained using a polynomial-derivative method in which peak positions and intensities are determined from the point at which the first derivative of emission intensity crosses the wavelength axis.

#### *Extrinsic fluorescence spectroscopy*

The dye 8-Anilino-1-naphthalene sulfonate (ANS) stock solution at  $1.0 \text{ M}$  concentration was prepared in dimethylformide

and then diluted with water to  $20 \text{ mM}$ . Eleven  $\mu\text{l}$  of  $20 \text{ mM}$  ANS were added to  $1.0 \text{ ml}$  of  $0.2 \text{ mg/ml}$  of *Sm-TSP-2* under each pH condition. ANS fluorescence spectra in the presence of *Sm-TSP-2* were collected using the PTI spectrofluorometer. An excitation wavelength of  $375 \text{ nm}$  was used, and spectra from  $400\text{--}600 \text{ nm}$  were collected every  $2.5 \text{ }^\circ\text{C}$  from  $10\text{--}87.5 \text{ }^\circ\text{C}$  with the slit width for both excitation and emission set at  $1.0 \text{ nm}$ . A spectrum of the buffer containing ANS was subtracted from each spectrum prior to data analysis using Microsoft Excel software. Maximum fluorescence intensities were plotted as a function of temperature to evaluate binding of ANS to the protein.

#### *Empirical phase diagram*

CD, tyrosine fluorescence intensity and ANS fluorescence intensity spectral data were used to generate an empirical phase diagram (EPD). The EPD technique is a vector-based multidimensional analysis method used for summarizing large data sets from a variety of biophysical techniques. For every combination of pH and temperature at which measurements were taken, a 3-dimensional vector was created. The assignment to each vector of a different color (red, green, and blue) produces a combination of unique colors representative of a particular structural state of the protein. Although the color itself has no physical meaning, a change in color in the EPD represents a structural change within the protein molecule, in this case as a function of solution pH and temperature.<sup>18,40</sup>

#### *Protein stability screening using a GRAS excipient library*

The *Sm-TSP-2* protein at around approximately  $1.0 \text{ mg}/\text{mL}$  was dialyzed against  $10 \text{ mM}$  imidazole buffer, pH 7.0 containing  $0.145 \text{ M}$  sodium chloride. Concentrated solutions of GRAS (generally regarded as safe) excipients were prepared in the imidazole buffer, and the pH was adjusted to pH 7.0. The *Sm-TSP-2* protein was mixed with the concentrated excipient solutions to adjust the *Sm-TSP-2* final protein concentration to  $0.2 \text{ mg}/\text{mL}$  and excipients to selected concentrations. Tyrosine fluorescence intensity was measured as previously described. Fluorescence intensity was normalized between 0 and 100 using the minimal fluorescence intensity as 0 and the maximal fluorescence intensity as 100 in the transition phase. The thermal unfolding ( $T_m$ ) values of the protein in the various solutions were determined as the temperature at which 50% of the normalized change intensity occurs.

#### **Disclosure of Potential Conflicts of Interest**

No potential conflicts of interest were disclosed.

## References

- King CH. Parasites and poverty: the case of schistosomiasis. *Acta Trop* 2010; 113:95-104; PMID:19962954; <http://dx.doi.org/10.1016/j.actatropica.2009.11.012>
- Gryseels B. Schistosomiasis. *Infect Dis Clin North Am* 2012; 26:383-97; PMID:22632645; <http://dx.doi.org/10.1016/j.idc.2012.03.004>
- Brindley PJ, Hotez PJ. Break Out: urogenital schistosomiasis and *Schistosoma haematobium* infection in the post-genomic era. *PLoS Negl Trop Dis* 2013; 7:e1961; PMID:22802974; <http://dx.doi.org/10.1371/journal.pntd.0001961>
- Hotez PJ. The London Declaration: a tipping point for the world's poor. *Huffington Post* 2012. [http://www.huffingtonpost.com/peter-hotez-md-phd/london-declaration-ntds\\_b\\_1237098.html](http://www.huffingtonpost.com/peter-hotez-md-phd/london-declaration-ntds_b_1237098.html)
- Riveau G, Deplanque D, Remoué F, Schacht AM, Vodougnon H, Capron M, et al. Safety and immunogenicity of rSh28GST antigen in humans: phase I randomized clinical study of a vaccine candidate against urinary schistosomiasis. *PLoS Negl Trop Dis* 2012; 6:e1704; PMID:22802974; <http://dx.doi.org/10.1371/journal.pntd.0001704>
- Ramos CR, Spisni A, Oyama S Jr, Sforça ML, Ramos HR, Vilar MM, et al. Stability improvement of the fatty acid binding protein Sm14 from *S. mansoni* by Cys replacement: structural and functional characterization of a vaccine candidate. *Biochim Biophys Acta* 2009; 1794:655-62; PMID:19150418; <http://dx.doi.org/10.1016/j.bbapap.2008.12.010>
- Loukas A, Tran M, Pearson MS. Schistosome membrane proteins as vaccines. *Int J Parasitol* 2007; 37:257-63; PMID:17222846; <http://dx.doi.org/10.1016/j.ijpara.2006.12.001>
- Tran MH, Pearson MS, Bethony JM, Smyth DJ, Jones MK, Duke M, et al. Tetraspanins on the surface of *Schistosoma mansoni* are protective antigens against schistosomiasis. *Nat Med* 2006; 12:835-40; PMID:16783371; <http://dx.doi.org/10.1038/nm1430>
- Tran MH, Freitas TC, Cooper L, Gaze S, Gatton ML, Jones MK, et al. Suppression of mRNAs encoding tegument tetraspanins from *Schistosoma mansoni* results in impaired tegument turnover. *PLoS Pathog* 2010; 6:e1000840; PMID:20419145; <http://dx.doi.org/10.1371/journal.ppat.1000840>
- Lindblad EB. Are mineral adjuvants triggering TLR2/TLR4 on dendritic cells by a secondary cascade reaction in vivo through the action of heat shock proteins and danger signals? *Vaccine* 2006; 24:697-8; PMID:16129524; <http://dx.doi.org/10.1016/j.vaccine.2005.07.076>
- Jones LS, Peek LJ, Power J, Markham A, Yazzie B, Middaugh CR. Effects of adsorption to aluminum salt adjuvants on the structure and stability of model protein antigens. *J Biol Chem* 2005; 280:13406-14; PMID:15684430; <http://dx.doi.org/10.1074/jbc.M500687200>
- Bai SF, Cai DZ, Li X, Chen XX. Parasitic castration of *Plutella xylostella* larvae induced by polydnaviruses and venom of *Cotesia vestalis* and *Diadegma semiclausum*. *Arch Insect Biochem Physiol* 2009; 70:30-43; PMID:18949808; <http://dx.doi.org/10.1002/arch.20279>
- Dong A, Jones LS, Kerwin BA, Krishnan S, Carpenter JF. Secondary structures of proteins adsorbed onto aluminum hydroxide: infrared spectroscopic analysis of proteins from low solution concentrations. *Anal Biochem* 2006; 351:282-9; PMID:16460655; <http://dx.doi.org/10.1016/j.ab.2006.01.008>
- Capelle MA, Brügger P, Arvinte T. Spectroscopic characterization of antibodies adsorbed to aluminium adjuvants: correlation with antibody vaccine immunogenicity. *Vaccine* 2005; 23:1686-94; PMID:15705473; <http://dx.doi.org/10.1016/j.vaccine.2004.09.031>
- Soliakov A, Kelly IF, Lakey JH, Watkinson A. Anthrax sub-unit vaccine: the structural consequences of binding rPA83 to Alhydrogel®. *Eur J Pharm Biopharm* 2012; 80:25-32; PMID:21964315; <http://dx.doi.org/10.1016/j.ejpb.2011.09.009>
- Bond MD, Panek ME, Zhang Z, Wang D, Mehndiratta P, Zhao H, et al. Evaluation of a dual-wavelength size exclusion HPLC method with improved sensitivity to detect protein aggregates and its use to better characterize degradation pathways of an IgG1 monoclonal antibody. *J Pharm Sci* 2010; 99:2582-97; PMID:20039394
- Harn N, Allan C, Oliver C, Middaugh CR. Highly concentrated monoclonal antibody solutions: direct analysis of physical structure and thermal stability. *J Pharm Sci* 2007; 96:532-46; PMID:17083094; <http://dx.doi.org/10.1002/jps.20753>
- Kueltzo LA, Ersoy B, Ralston JP, Middaugh CR. Derivative absorbance spectroscopy and protein phase diagrams as tools for comprehensive protein characterization: a bGCSF case study. *J Pharm Sci* 2003; 92:1805-20; PMID:12949999; <http://dx.doi.org/10.1002/jps.10439>
- Zheng K, Middaugh CR, Siahaan TJ. Evaluation of the physical stability of the EC5 domain of E-cadherin: effects of pH, temperature, ionic strength, and disulfide bonds. *J Pharm Sci* 2009; 98:63-73; PMID:18428798; <http://dx.doi.org/10.1002/jps.21418>
- Smith GJ, Melhuish WH. Relaxation and quenching of the excited states of tryptophan in keratin. *J Photochem Photobiol B* 1993; 17:63-8; PMID:7679440; [http://dx.doi.org/10.1016/1011-1344\(93\)85008-V](http://dx.doi.org/10.1016/1011-1344(93)85008-V)
- Stryer L. The interaction of a naphthalene dye with apomyoglobin and apohemoglobin. A fluorescent probe of non-polar binding sites. *J Mol Biol* 1965; 13:482-95; PMID:5867031; [http://dx.doi.org/10.1016/S0022-2836\(65\)80111-5](http://dx.doi.org/10.1016/S0022-2836(65)80111-5)
- Matulis D, Lovrien R. 1-Anilino-8-naphthalene sulfonate anion-protein binding depends primarily on ion pair formation. *Biophys J* 1998; 74:422-9; PMID:9449342; [http://dx.doi.org/10.1016/S0006-3495\(98\)77799-9](http://dx.doi.org/10.1016/S0006-3495(98)77799-9)
- Gasymov OK, Glasgow BJ. ANS fluorescence: potential to augment the identification of the external binding sites of proteins. *Biochim Biophys Acta* 2007; 1774:403-11; PMID:17321809; <http://dx.doi.org/10.1016/j.bbapap.2007.01.002>
- Peek LJ, Brandau DT, Jones LS, Joshi SB, Middaugh CR. A systematic approach to stabilizing EBA-175 RII-NG for use as a malaria vaccine. *Vaccine* 2006; 24:5839-51; PMID:16735084; <http://dx.doi.org/10.1016/j.vaccine.2006.04.067>
- Chen CK, Chen PK, Chiu WT, Cheng WD, Tsui PH. Comparison of high-resolution computed tomography with conventional injection fitting method for fabricating hearing aid shells. *Otolaryngology-head and neck surgery: official journal of American Academy of Otolaryngology-Head Neck Surg* 2012; 147:170-2; <http://dx.doi.org/10.1177/0194599812440539>
- Burton L, Gandhi R, Duke G, Paborji M. Use of microcalorimetry and its correlation with size exclusion chromatography for rapid screening of the physical stability of large pharmaceutical proteins in solution. *Pharm Dev Technol* 2007; 12:265-73; PMID:17613890; <http://dx.doi.org/10.1080/10837450701212610>
- Gietz U, Alder R, Langguth P, Arvinte T, Merkle HP. Chemical degradation kinetics of recombinant hirudin (HV1) in aqueous solution: effect of pH. *Pharm Res* 1998; 15:1456-62; PMID:9755900; <http://dx.doi.org/10.1023/A:1011918108849>
- Goolcharan C, Cleland JL, Keck R, Jones AJ, Borchardt RT. Comparison of the rates of deamidation, diketopiperazine formation and oxidation in recombinant human vascular endothelial growth factor and model peptides. *AAPS PharmSci* 2000; 2:E5; PMID:11741221
- Li S, Patapoff TW, Overcashier D, Hsu C, Nguyen TH, Borchardt RT. Effects of reducing sugars on the chemical stability of human relaxin in the lyophilized state. *J Pharm Sci* 1996; 85:873-7; PMID:8863280; <http://dx.doi.org/10.1021/js950456s>
- Banks DD, Hamby DM, Scavezze JL, Siska CC, Stackhouse NL, Gadgil HS. The effect of sucrose hydrolysis on the stability of protein therapeutics during accelerated formulation studies. *J Pharm Sci* 2009; 98:4501-10; PMID:19388069; <http://dx.doi.org/10.1002/jps.21749>
- Gadgil HS, Bondarenko PV, Pipes G, Rehder D, McAuley A, Perico N, et al. The LC/MS analysis of glycation of IgG molecules in sucrose containing formulations. *J Pharm Sci* 2007; 96:2607-21; PMID:17621682; <http://dx.doi.org/10.1002/jps.20966>
- Tsai PK, Volkin DB, Dabora JM, Thompson KC, Bruner MW, Gress JO, et al. Formulation design of acidic fibroblast growth factor. *Pharm Res* 1993; 10:649-59; PMID:7686672; <http://dx.doi.org/10.1023/A:1018939228201>
- Thakkar SV, Joshi SB, Jones ME, Sathish HA, Bishop SM, Volkin DB, et al. Excipients differentially influence the conformational stability and pretransition dynamics of two IgG1 monoclonal antibodies. *J Pharm Sci* 2012; 101:3062-77; PMID:22581714; <http://dx.doi.org/10.1002/jps.23187>
- Plieskatt JL, Rezende WC, Olsen CM, Trefethen JM, Joshi SB, Middaugh CR, et al. Advances in vaccines against neglected tropical diseases: enhancing physical stability of a recombinant hookworm vaccine through biophysical and formulation studies. *Hum Vaccin Immunother* 2012; 8:765-76; PMID:22495115; <http://dx.doi.org/10.4161/hv.19726>
- Lee JC, Timasheff SN. The stabilization of proteins by sucrose. *J Biol Chem* 1981; 256:7193-201; PMID:7251592
- Kendrick BS, Chang BS, Arakawa T, Peterson B, Randolph TW, Manning MC, et al. Preferential exclusion of sucrose from recombinant interleukin-1 receptor antagonist: role in restricted conformational mobility and compaction of native state. *Proc Natl Acad Sci U S A* 1997; 94:11917-22; PMID:9342337; <http://dx.doi.org/10.1073/pnas.94.22.11917>
- Timasheff SN. Protein-solvent preferential interactions, protein hydration, and the modulation of biochemical reactions by solvent components. *Proc Natl Acad Sci U S A* 2002; 99:9721-6; PMID:12097640; <http://dx.doi.org/10.1073/pnas.122253999>
- Kamerzell TJ, Esfandiary R, Joshi SB, Middaugh CR, Volkin DB. Protein-excipient interactions: mechanisms and biophysical characterization applied to protein formulation development. *Adv Drug Deliv Rev* 2011; 63:1118-59; PMID:21855584; <http://dx.doi.org/10.1016/j.addr.2011.07.006>
- Carpenter JF, Crowe JH. The mechanism of cryoprotection of proteins by solutes. *Cryobiology* 1988; 25:244-55; PMID:3396389; [http://dx.doi.org/10.1016/0011-2240\(88\)90032-6](http://dx.doi.org/10.1016/0011-2240(88)90032-6)
- Maddux NR, Joshi SB, Volkin DB, Ralston JP, Middaugh CR. Multidimensional methods for the formulation of biopharmaceuticals and vaccines. *J Pharm Sci*. Forthcoming 2011; PMID:21647886; <http://dx.doi.org/10.1002/jps.22618>